The 2023 World Congress on
Advances in Structural Engineering and Mechanics (ASEM23)
GECE, Seoul, Korea, August 16-18, 2023

Patch loading resistance prediction of plate girders with multiple longitudinal stiffeners using machine learning

Carlos Graciano[1)*], Ahmet-Emin Kurtoglu[2)], Balázs Kövesdi [3)], Euro Casanova[4)]

[1)] *Departamento de Ingeniería Civil, Universidad Nacional de Colombia, Facultad de Minas, Sede Medellín, A.A. 75267, Medellín, Colombia*
[2)] *Department of Civil Engineering, Igdir University, Şehit Bülent Yurtseven Campus, 76000 Igdir, Turkey*
[3)] *Department of Structural Engineering, Budapest University of Technology and Economics, H-1111 Budapest, Műegyetem rkp. 3, Hungary*
[4)] *Departamento Ingeniería Civil y Ambiental, Universidad del Bío-Bío, Avenida Collao 1202, Concepción, Código Postal 4051381, Chile*
1) cagracianog@unal.edu.co

ABSTRACT

This paper is aimed at investigating the effect of multiple longitudinal stiffeners on the patch loading resistance of slender steel plate girders. Firstly, a numerical study is conducted through geometrically and materially nonlinear analysis with imperfections included (GMNIA), the model is validated with experimental results taken from the literature. The structural responses of girders with multiple longitudinal stiffeners are compared to the one of girders with a single longitudinal stiffener. Thereafter, a patch loading resistance model is developed through machine learning (ML) using symbolic regression (SR). An extensive numerical dataset covering a wide range of bridge girder geometries is employed to fit the resistance model using SR. Finally, the performance of the SR prediction model is evaluated by comparison of the resistances predicted using available formulae from the literature.

1. INTRODUCTION

In recent years, there have been a growing interest on the resistance of plate girders stiffened with one single longitudinal stiffener. Graciano (2015) conducted an

*Corresponding author, Professor, E-mail: cagracianog@unal.edu.co
[a] Ph.D., E-mail: aemin.kurtoglu@igdir.edu.tr
[b] Ph.D., E-mail: kovesdi.balazs@emk.bme.hu
[c] Ph.D., E-mail: ecasanova@ubiobio.cl

extensive literature review concerning studies dealing with critical buckling load and resistance models for steel plate girders with a single stiffener subject to patch loading. Shimizu et al. (1987) conducted an experimental investigation on the strength of plate girders subject to patch loading. A test was performed on a girder subjected to combined patch loading and bending with two stiffeners welded in the compression zone. Benedetti and Dall'Aglio (2011, 2012) also performed numerical studies on the patch load resistance of steel plate girders varying the location of two longitudinal stiffeners placed beneath the loaded flange. Loaiza et al. (2017a) using nonlinear finite analysis studied the influence of the bearing length on the patch loading resistance of multiple stiffened girders, and the response was compared to that of girders with single open and closed section stiffeners (Loaiza et al. 2017b). Kövesdi et al. (2018) conducted an experimental investigation on the patch loading resistance of girders with multiple longitudinal stiffeners with small bending and torsional stiffness (weak stiffeners). A numerical study was also conducted to investigate the effect of hand-defined imperfection shapes. Kövesdi (2018) conducted an extensive numerical investigation on the resistance to patch loading of plate girders with single and multiple longitudinal stiffeners. This investigation considered the effect of several geometrical parameters, placing particular interest in the loading length, the rigidity of the stiffener, and the shape of the initial geometric imperfections. From the numerical results, an expression for the elastic buckling load was proposed for girders with multiple strong stiffeners. Loaiza et al. (2019a, 2019b) obtained similar results to those found by Kövesdi (2018) imposing a nodal line along the stiffener location (i.e. restricting the displacements but allowing all rotations). Kövesdi and Dunai (2022) proposed an improved formulation for the yield load length of plate girders having multiple longitudinal stiffeners subjected to patch loading.

Computer science has evolved towards artificial intelligence (AI) dealing with the formation of smart machines and building algorithms that mimic human behavior, and employ them to solve engineering challenges (Salehi and Burgueño 2018). Over the last decades, AI has demonstrated to be an efficient alternative compared to classical modeling techniques in a number of structural engineering applications (Cevik et al. 2015, Salehi and Burgueño 2018, Sun et al. 2021, Thai 2022, Tapeh and Naser 2023). In previous studies, SR have been employed to predict the resistance to patch loading of aluminum extrusions (Kurtoglu et al. 2022), and stainless steel girders (Graciano et al. 2021).

In this paper the effect of multiple longitudinal stiffeners on the structural response of slender steel plate girders subjected to patch loading is investigated. A numerical study is performed through geometrically and materially nonlinear analysis with imperfections included (GMNIA). This model is validated against experimental results reported in the literature. The structural response of the multi-stiffened girders is compared to that of girders with single longitudinal stiffener. Significant differences are attained in the resistances and stress distributions. Then, a resistance prediction model is developed through machine learning (ML) using symbolic regression (SR). An extensive numerical dataset is employed to fit the corresponding prediction model. This dataset covers a wide range of bridge girder geometries. At the end, the accuracy of the proposed model is assessed against an existing formula in the literature. The comparison of the proposed model with existing models reveals that, despite its simplicity, the model can provide reasonably accurate predictions.

2. NUMERICAL MODEL

Fig. 1 shows a schematic view and corresponding notation for a plate girder with multiple longitudinal stiffeners with open-sections subject to patch loading. The numerical models were elaborated using shell S181 elements in ANSYS (ANSYS 2018). Geometrically and materially nonlinear analyses with imperfections included (GMNIA) were conducted to determine the patch loading resistance of the girders

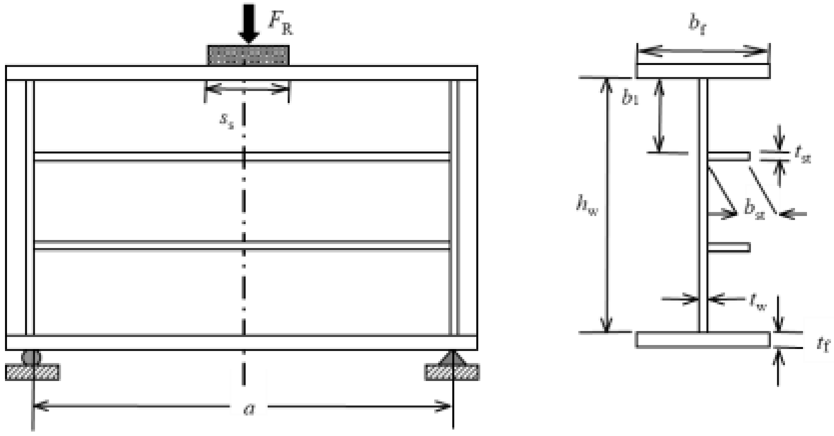

Fig. 1. A plate girder with two equi-spaced longitudinal stiffeners subject to patch loading.

Table 1. Geometry and results of the tested girders with multiple longitudinal stiffeners (Kövesdi et al. 2018).

Girder	n_s	s_s (mm)	b_1 (mm)	γ_s	f_{yw} (MPa)	f_{yf} (MPa)	F_R^{EXP} (kN)	F_R^{FEM} (kN)	$\frac{F_R^{FEM}}{F_R^{EXP}}$
#1	-	200	-	-	286	288	206.4	236.64	1.16
#2	2	200	165	27.27	318	268	258.4	276.48	1.07
#3	3	200	123	27.27	311	266	270.9	277.74	1.03
#4	3	200	123	80.55	314	283	320.4	323.56	1.01
#5	-	100	-	-	308	272	180.2		
#6	2	100	165	27.27	343	262	214.3	227.14	1.06
#7	3	100	123	27.27	299	285	218.4	212.51	0.97
#8	3	100	123	80.55	311	288	223.8	227.53	1.02

Table 1 presents the geometry and material properties of the girders with multiple longitudinal stiffeners tested by Kövesdi et al. (2018). All girders have the same dimensions: a = 990mm, h_w = 500mm, t_w = 4mm, b_f = 150mm, t_f = 10mm. Two stiffeners with different sizes were employed 40 mm x4 mm (γ_s = 27.27) and 60mm x4mm (γ_s = 80.55) flat plate stiffeners. Stiffener rigidities were calculated using Eq. (11).

Material nonlinearities were considered in the model assuming a perfectly elastoplastic material for all girders components (flanges, web and stiffeners), the Young's modulus was set to E=200 GPa, and the Poisson's ratio was set to v=0.3. Fig. 3 shows a schematic view of the geometry and stiffener configuration of the tested girders (Kövesdi et al. 2918). Initial geometric imperfections were introduced employing the first buckling mode with a maximum amplitude of h_w/200 (EC3:1-5 2006).

In a similar manner as in the test setup, the load was transferred to the upper flange through the nodes over a length s_s, only the vertical displacement in these nodes were allowed, i.e. the displacements in the out-of-plane direction and all rotations were restrained. Furthermore, the load was applied through an arc-length based incremental method to trace the response in the postbuckling region. At the girder ends, simply supported conditions were established. Transverse stiffeners above the vertical supports of the girder were also laterally supported to avoid lateral torsional buckling, allowing only their in-plane rotation.

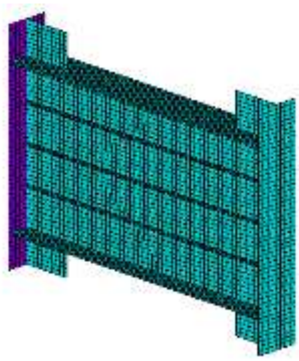

Fig. 2. Final mesh for girders with 3 longitudinal stiffeners.

A convergence analysis was performed with three average element sizes: 10, 14, and 15 mm, respectively. Fig. 2 shows the final mesh with an element size of 15 mm for a girder with 3 longitudinal stiffeners. As seen in Table 1, a very close agreement between the experimental and numerical resistances was attained with an average value of 1.05.

3. STRUCTURAL RESPONSE OF MULTIPLE STIFFENED GIRDERS

From the tests, it is clearly observed that the patch loading resistance of plate girders increases with the number of stiffeners. Nevertheless, in the experiments conducted by Kövesdi et al. (2018), two cases commonly found in practice were not analyzed, a girder with a single longitudinal stiffener placed at $0.2h_w$, and a girder with two longitudinal stiffeners, one at $0.2h_w$ and a second at $0.8h_w$. The latter configuration is frequently employed to increase the bending resistance of steel bridge girders for sagging and bending moments under in-service conditions.

3.1. Parametric study

In this section, a parametric study is conducted to further investigate the influence of the presence of multiple stiffeners on the resistance to patch loading. The two cases mentioned above are included in the analysis, and two additional cases are also investigated (girders with 4 and 5 stiffeners). The geometry and material properties of Girder #4 in Table 1 were used throughout this study. Table 2 presents the results obtained numerically in the parametric study.

Table 2. Results for the girders used in the parametric study.

Case	n_s	b_1 (mm)	γ_s	h_{wi}/t_w	F_R^{FEM} (kN)
I	0	-	-	-	250.73
II	1*	100.0	80.55	100.0	295.33
III	2**	100.0	80.55	75.00	296.00
IV	2	166.7	80.55	41.67	308.72
V	3	125.0	80.55	31.25	323.62
VI	4	100.0	80.55	25.00	337.07
VII	5	83.3	80.55	20.83	347.23

* Girder with a single stiffener placed a $b_1 = 0.20h_w$.
** Girder with two stiffeners placed a $b_1 = 0.20h_w$ & $0.80h_w$.

Table 2 presents threes cases with b_1=100mm corresponding to $b_1 = 0.20h_w$, the effect of the stiffener placed beneath the load is the same for Cases II and III, but for Case IV with four longitudinal stiffeners is different, since a larger increase in the resistance is attained. It demonstrates that the response of plates girders with a single stiffener change with respect to that of girders with multiple stiffeners for the stiffener location.

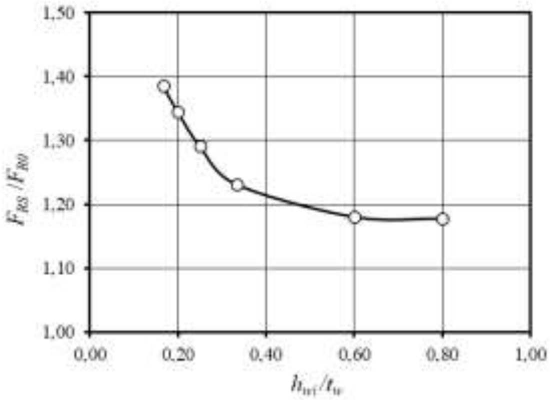

Fig. 3. Ratio F_{RS}/F_{R0} versus the slenderness of the larger panel (h_{wi}/t_w).

Fig. 3 shows a comparison of the computed resistances in Table 2 for unstiffened F_{R0} and stiffened girders F_{RS}. Comparing the resistance between the unstiffened girder (F_{R0}= 250.7kN) and the girder with two equi-spaced stiffeners (F_{RS}= 308.7kN) there is an increase of 23% (Fig. 3). For the girder with five equi-spaced stiffeners (F_{RS}= 347.2kN) the resistance increases 39% with respect to the unstiffened web. It seems that the slenderness of the largest web panel ($h_{\mathrm{wi}}/t_{\mathrm{w}}$) affect the response of the girders. As seen in Fig. 3, the resistance of the stiffened girders decreases with an increasing slenderness ratio $h_{\mathrm{wi}}/t_{\mathrm{w}}$.

3.2. Stress distribution plots

Fig. 4 plots the von Mises stress distribution at ultimate load level for the cases mentioned above. For Case II and III (Figs. 7a and 7b), two highly stressed areas are visibly defined, one beneath the load and another below the longitudinal stiffener within the subpanel with larger slenderness. For Cases IV to VII (Figs. 7c to 7f), failure occurs in the directly loaded subpanel. Naturally, the out-of-plane displacements in the web is highly restricted due to the presence of multiple stiffeners.

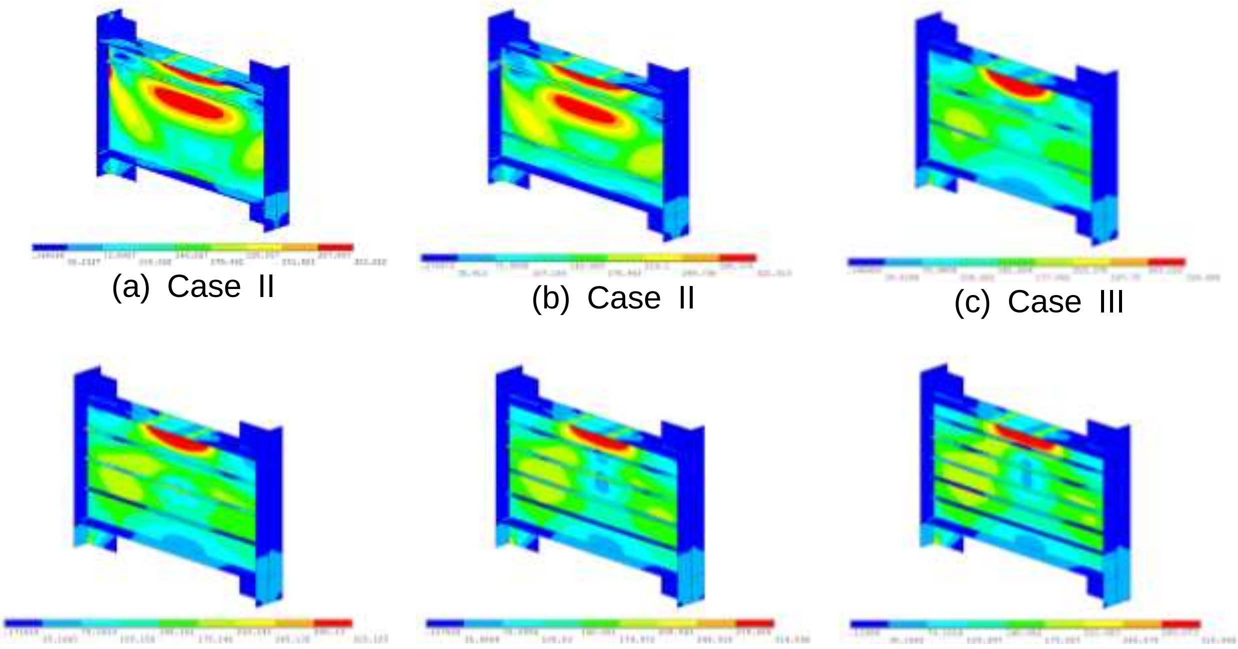

(a) Case II (b) Case II (c) Case III

(d) Case IV (e) Case V (f) Case VI

Fig. 4. Plots of von Mises stress distribution (MPa) for girders with multiple stiffeners.

4. Resistance model for multiple stiffened girders

Recently, Kövesdi and coworkers (Kövesdi et al. 2018, Kövesdi 2018, Kövesdi and Dunai 2022) have conducted experimental, numerical and theoretical research to investigate the effect of multiple longitudinal stiffeners on the patch loading resistance of slender steel plate girders. Kövesdi (2018) originally proposed a prediction resistance model based on the EN1993-1-5 guidelines (EC3:1-5 2006), and the model was further improved by Kövesdi and Dunai (2022). This resistance model is summarized as follows, the resistance to patch loading for steel plate girders with multiple longitudinal stiffeners F_{RD} is

$$F_{\mathrm{RD}} = \chi_{\mathrm{F}} \frac{l_{\mathrm{y}}\, f_{\mathrm{yw}}\, t_{\mathrm{w}}}{\gamma_{\mathrm{M1}}} \tag{1}$$

in which χ_{F} is the reduction factor due to local buckling, l_{y} is the effective loaded length, f_{yw} is the web yield strength of the web, t_{w} is the web thickness, and γ_{M1} is the partial safety factor. In Eq. (1), the reduction factor χ_{F} is determined using the imperfection factor α_{F0}, the plateau length $\bar{\lambda}_{\mathrm{F0}}$, and the slenderness parameter $\bar{\lambda}_{\mathrm{F}}$

$$\chi_{\mathrm{F}} = \frac{1.0}{\phi_{\mathrm{F}} + \sqrt{\phi_{\mathrm{F}}^2 - \bar{\lambda}_{\mathrm{F}}}} \leq 1.0 \tag{2}$$

$$\phi_F = \frac{1}{2}\left[1 + \alpha_{\mathrm{F0}}\left(\bar{\lambda}_{\mathrm{F}} - \bar{\lambda}_{\mathrm{F0}}\right) + \bar{\lambda}_{\mathrm{F}}\right] \tag{3}$$

$$\bar{\lambda}_{\mathrm{F}} = \sqrt{\frac{l_{\mathrm{y}}\, f_{\mathrm{yw}}\, t_{\mathrm{w}}}{F_{\mathrm{cr}}}} \tag{4}$$

Kövesdi (2018) calibrated the resistance function for patch loading and multiple longitudinal stiffeners attaining α_{F0}=0.75, $\bar{\lambda}_{\mathrm{F0}}$=0.50, for a partial safety factor γ_{M1}=1.10. More recently, Kövesdi and Dunai (2022) proposed the following expressions for the effective loaded length l_{y}

$$l_y = s_s + 2t_f\left[\sqrt{\frac{t_w}{t_f}\left(0.5\frac{b_1}{t_w} - 10\right)}\right] \quad \text{for} \quad 20 < \frac{b_1}{t_w} \leq 70 \tag{5a}$$

$$l_{\mathrm{y}} = s_{\mathrm{s}} + 2t_{\mathrm{f}}\left[\sqrt{\frac{t_{\mathrm{w}}}{t_{\mathrm{f}}} 0.2 \frac{b_1}{t_{\mathrm{w}}}\frac{b_1}{s_{\mathrm{s}}}}\right] \quad \text{for} \quad \frac{b_1}{t_{\mathrm{w}}} > 70 \tag{5b}$$

For girders with multiple strong stiffeners, the critical buckling load F_{cr} is

$$F_{\mathrm{cr}} = k_{\mathrm{F}}\frac{\pi^2 E}{12\,(1-\nu^2)}\frac{t_{\mathrm{w}}^3}{b_1} = 0.9\, E\, k_{\mathrm{F}}\frac{t_{\mathrm{w}}^3}{b_1} \tag{6}$$

where E= 200GPa is the Young's modulus, ν=0.3 is the Poisson's ratio, and the buckling coefficient k_{F} is

$$k_{\mathrm{F}} = 4 + 1.5\frac{s_{\mathrm{s}}}{b_1} \tag{7}$$

A previous version of Eq. (7) was initially developed by Kövesdi (2018) for strong stiffeners, in which the flexural rigidity γ_s of the stiffener fulfills

$$\gamma_s > 13\left(\frac{a}{h_{\mathrm{w}}}\right)^3 + 210\left(0.3 - \frac{b_1}{a}\right) \tag{8}$$

In Eq. (8), the flexural rigidity of the stiffener is calculated with

$$\gamma_{\mathrm{s}} = 10.9\frac{I_{\mathrm{sl}}}{h_{\mathrm{w}} t_{\mathrm{w}}^3} \leq 13\left(\frac{a}{h_{\mathrm{w}}}\right)^3 + 210\left(0.3 - \frac{b_1}{a}\right) \tag{9}$$

The parameter I_{sl} represents the second moment of area of the longitudinal stiffener itself and an effective web plate part with a width of $15\varepsilon t_{\mathrm{w}}$ on both sides of the stiffener (Fig. 5).

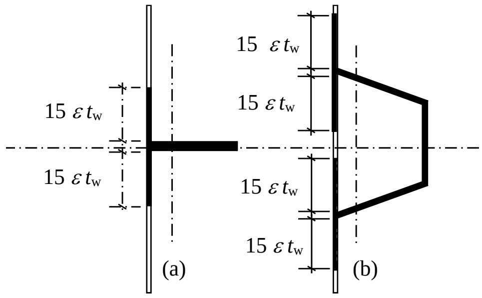

Fig. 5. Effective cross-section (a) open section stiffener (OSS), and (b) closed section stiffener (CSS).

5. Machine learning (ML) model

5.1 Data collection

In this study, a numerical database developed by Kövesdi (2018) is employed to develop the ML model. The study was conducted using closed and open-section stiffeners (Fig. 6). Originally, the database was composed of 900 simulations including weak and strong stiffeners. This database was reduced to 576 simulations (423 with CSS and 153 with OSS) using only strong stiffeners. It is worth pointing out that all strong stiffeners fulfil Eq. (8). In this manner, the flexural rigidity is implicitly considered, the relative stiffness of the longitudinal stiffeners γ_s was set between 60 and 4600, calculated according to Eq. (9).

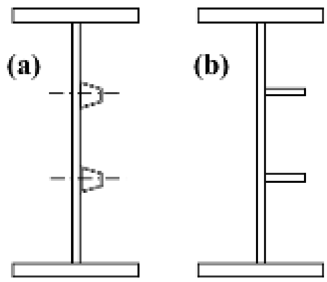

Fig. 6. Plate girders with: (a) CSS, and (b) OSS.

Table 3. Ranges of parameters analyzed in the parametric study (Kövesdi 2018).

St		a (mm)	h_w (mm)	t_w (mm)	b_f (mm)	t_f (mm)	s_s (mm)	b_1 (mm)
CSS	Min	2400	1000	3	260	12	120	250
	Max	6000	4000	20	600	60	2000	1000
OSS	Min	1000	500	4	150	10	100	125
	Max	1500	1100	10	220	16	400	365

Table 3 summarizes the parameters investigated with their minimum and maximum values. This database covers a large range of girder geometries which are commonly applied in bridge design praxis. After combining the input parameters, various geometric ratios were attained as shown in Table 4.

Table 4. Ranges of inputs in parametric database.

		a/h_w	s_s/b_1	b_1/t_w	b_f/t_f	s_s/h_w	b_1/h_w
CSS	Min	1	0.29	31.25	8.33	0.071	0.20
	Max	2.4	4.57	180	28.57	1.60	0.35
OSS	Min	1.25	0.38	27.67	13.75	0.125	0.33
	Max	2.0	2.4	60.83	18.33	0.6	0.18

Fig. 7 shows sensitivity plots for the ratio $F_R^{FEM}/f_{yw}t_w^2$ with respect to various geometric ratios for girders with multiple longitudinal CSS: a/h_w (Fig. 7a); b_1/t_w (Fig. 7b); t_f/t_w (Fig. 7c); b_f/t_f (Fig. 7d); b_f/t_w (Fig. 7e); and s_s/b_1 (Fig. 7f). In theses plots, it is noteworthy that the ratio $F_R^{FEM}/f_{yw}t_w^2$ is highly correlated to the geometric ratio s_s/b_1. Similar trends were observed for girders with OSS.

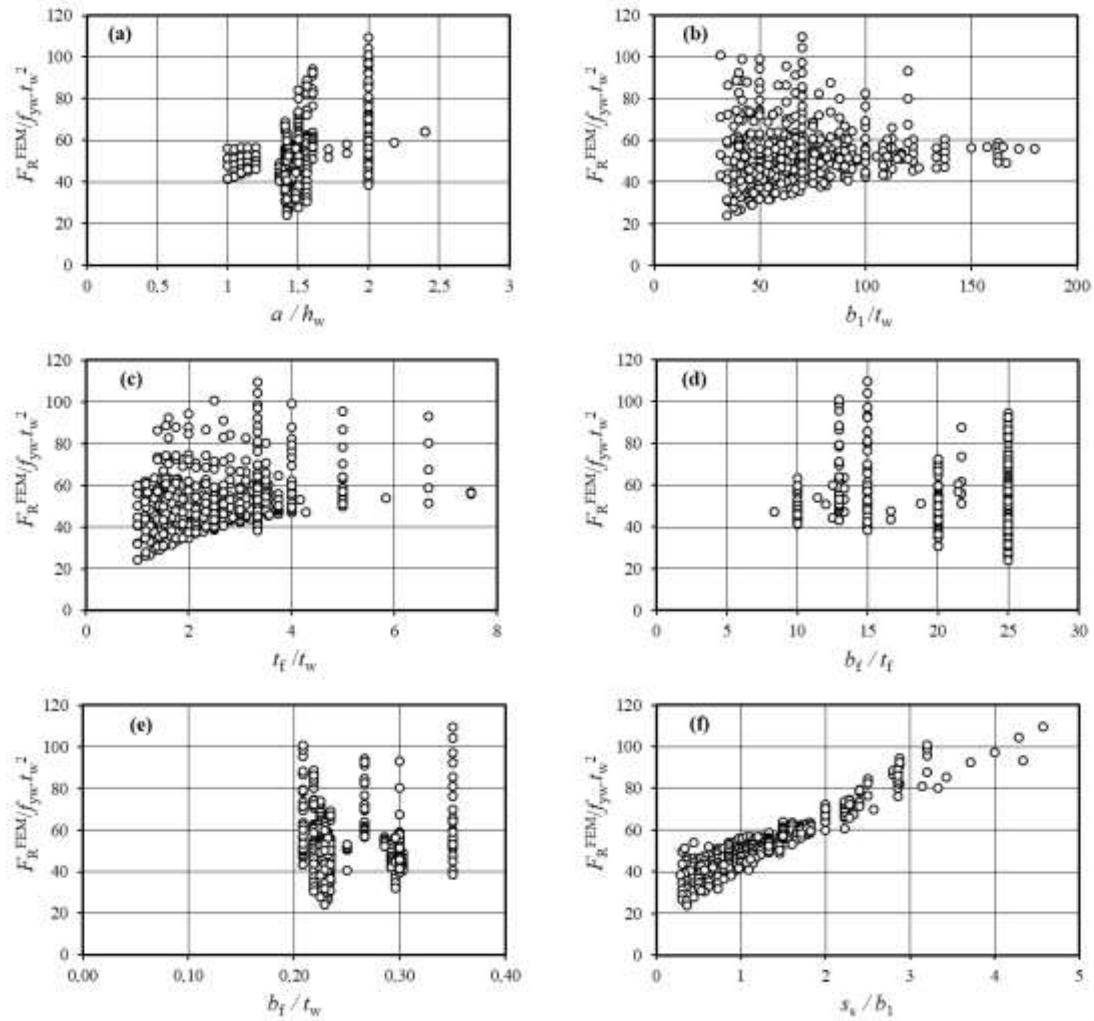

Fig. 7. Sensitivity analysis for girders stiffened with CSS.

5.2. Symbolic Regression (SR)

Symbolic Regression (SR) is a function discovery approach derived from genetic programming (GP) in which a space of mathematical expressions is searched by utilizing multivariate datasets. SR exhibits some advantages such as: performing a simultaneous search for equations and parameters for the addressed modeling problem, producing equations by recombining previously formed sub-expressions having potential to contribute to overall accuracy, and allowing the user to select mathematical building blocks (constants, arithmetic operators, logical and mathematical functions). In the end, the expressions with best-fitting metrics are maintained for further use and the remaining expressions are eliminated. This iterative process continues until desired levels of accuracy and simplicity are attained. Subsequently, the expressions with the best-fitting abilities are returned (Schmidt and Lipson 2005, 2007). To evaluate the SR model, two statistical metrics including the correlation coefficient (R^2), and the root mean square error ($RMSE$) are used. These metrics are defined as follows:

$$RMSE = \sqrt{\frac{\sum_{i=1}^{N}(o_i - t_i)^2}{N}} \tag{10}$$

where *N* is the total number of data, t_i is the predicted value of *ith* data, o_i is the observed value of i^{th} data. Eq. (13) gives the formulation for the coefficient of correlation, R^2, which is a measure of fitness level between actual and predicted values. Thus, it implies the existence of high correlations if R^2 approaches to 1.

$$R^2 = 1 - \left[\frac{\sum_{i=1}^{N}(o_i - t_i)^2}{\sum_{i=1}^{N}(o_i - o')^2}\right] \tag{11}$$

where o_i is the experimental value of i^{th} data, t_i is the predicted value of i^{th} data, o' is the average of actual values, and *N* is the total number of data used.

5.3. Development of SR model

Gplearn (2023) is an application programming interface (API) that expands the scikit-learn machine learning library to enable the implementation of Genetic Programming (GP) for symbolic regression (SR) in Python programming language. Accordingly, Gplearn (2023) was employed to develop a predictive model for patch loading resistance of slender I-girders with multiple longitudinal stiffeners. The approach involves representing potential solutions as trees, wherein intermediate nodes encode mathematical operations such as addition, subtraction, multiplication, division, among others, while terminal nodes represent the problem's constants and variables. The user-defined nodes are collectively referred to as building blocks. The fitness function is typically proportional to the absolute or squared error between the experimental data and the predicted values of a candidate solution. To favor more concise equations, parsimony modifications are implemented.

The patch loading resistance can be represented in terms of geometric ratios and the web's yield strength, as also stated by failure mechanism solutions in the literature (Graciano and Edlund 2003, Hajdin and Markovic 2012). Eq. (12) lists the parameters that have the greatest impact on the patch loading resistance of longitudinally stiffened girders.

$$F_{\mathrm{R}} = f\left(f_{\mathrm{yw}}, t_{\mathrm{w}}^{2}, \frac{a}{h_{\mathrm{w}}}, \frac{b_{\mathrm{f}}}{t_{\mathrm{f}}}, \frac{s_{\mathrm{s}}}{b_{1}}, \frac{b_{1}}{t_{\mathrm{w}}}, \frac{t_{\mathrm{f}}}{t_{\mathrm{w}}}\right) \quad (12)$$

The database used to fit F_{R} was described in Section 5. The objective is to develop a model that could predict the patch loading resistance of girders with multiple stiffeners. The dataset was subsequently partitioned into randomly-assigned training (75%) and testing (25%) sets. To randomize the datasets, each row in the datasheet was assigned a random index number, and the datasheet was sorted in ascending order based on this index column. The training set is utilized by the algorithm to create expressions and assess the resulting models according to the fitness function. The variables used herein for SR modeling are shown in Table 4.

Table 4. Parameters used in SR modeling

Variables		Factors	Units
y	F_R^{FEM}	Resistance computed by FEM	kN
x_1	f_{yw}	Web yield strength	MPa
x_2	t_{w}	Web thickness	mm
x_3	t_{f}	Flange thickness	mm
x_4	s_{s}	Length of patch load	mm
x_5	h_{w}	Web panel height	mm
x_6	a	Web panel length	mm
x_7	b_{f}	Flange width	mm
x_8	b_1	Distance of stiffener from upper flange	mm

Among several expressions developed by SR, Eq. (13) was selected for further investigation due to its superior performance in the least error compared to other candidate solutions.

$$F_{\mathrm{R}}^{SR} = 0.0226\, f_{\mathrm{yw}} t_{\mathrm{w}}^{2} \left(\frac{s_{\mathrm{s}} + 2t_{\mathrm{f}}}{b_{1}}\right)^{0.5449} \left(\frac{a}{h_{\mathrm{w}}}\right)^{0.1566} \left(\frac{b_{\mathrm{f}}}{t_{\mathrm{f}}}\right)^{0.0678} \left(\frac{b_{1}}{t_{\mathrm{w}}}\right)^{0.0982} \left(\frac{t_{\mathrm{f}}}{t_{\mathrm{w}}}\right)^{0.0509} \quad (13)$$

Symbolic regression provided simple yet effective equation that fits data generated from comprehensive numerical simulations of plate girders with multiple stiffeners.

5.4. Comparison and performance evaluation of proposed model

In this section, the performance of the proposed model –Eq. (13) – for slender steel girders with multiple stiffeners was evaluated. Fig. 8 compare the computed resistances by Kövesdi and Dunai (2022) with those obtained with the proposed SR model in Eq. (13), and obtained according the formulation presented in Section 5. Fig. 8 displays the scatter plot of the predicted values generated by the proposed model against the corresponding numerical values.

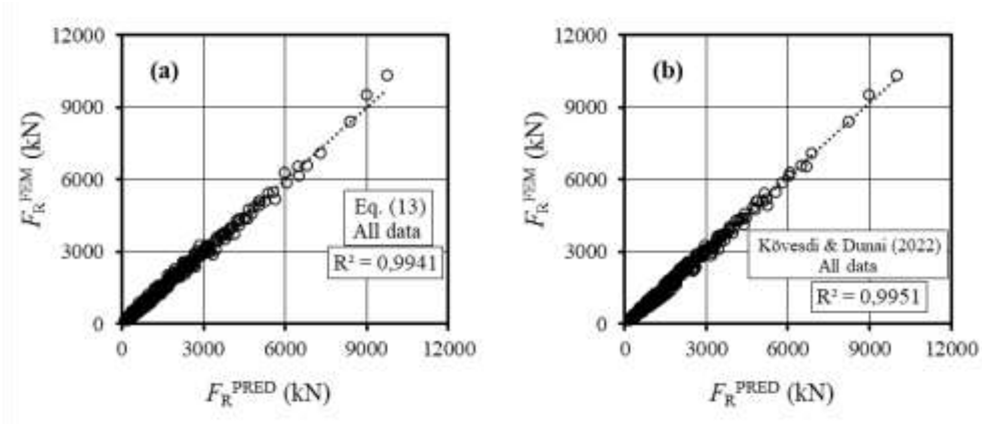

Fig. 8. Comparison between computed and predicted resistances.

Table 5. Accuracy of models.

	$F_R^{\text{Eqs. (1)–(7)}}$			$F_R^{\text{Eq. (13)}}$		
	Training	*Testing*	*Total*	*Training*	*Testing*	*Total*
Mean num./pred.	0.9868	1.0036	0.9997	1.0508	0.9966	1.0048
Std Dev.	0.0752	0.0802	0.0826	0.1050	0.0944	0.1097
COV	0.0762	0.0799	0.0826	0.0999	0.0947	0.1091
RMSE	94.1761	114.9390	102.8573	99.7631	114.1159	103.5106
R^2	0.9951	0.9950	0.9951	0.9941	0.9944	0.9941

Table 5 compares the statistical metrics of the method proposed by Kövesdi and Dunai (2022) and the proposed model in Eq. (13). Minor variances can be discerned in the numerical-to-predicted ratios, deviations, and error metrics.

6. CONCLUSIONS

This paper investigated the effect of multiple longitudinal stiffeners on the patch loading resistance of slender steel plate girders. The study was conducted numerically through GMNIA analyses using finite element simulations. The effect of multiple and single longitudinal stiffeners was investigated obtaining stress distribution plots. Different responses were observed for single and multi stiffened plate girder, hence these two types of stiffening should be analyzed separately.

A prediction resistance model was developed through machine learning using symbolic regression. The model was attained from the results of an extensive numerical dataset. The accuracy and applicability of the proposed model was assessed through comparison with an existing model as well as a sensitivity analysis. A good agreement was achieved between the predicted resistances using the SR approach a those predicted with formulae available in the literature.

REFERENCES

ANSYS. Ansys Release 19 Elements Reference, 2018.

Benedetti A, Dall'Aglio F. “Patch loading of longitudinally stiffened webs”. Bridge Maintenance, Safety, Management, Resilience and Sustainability - Proceedings of the Sixth International Conference on Bridge Maintenance, Safety and Management, 2012:1039–1046.

Çevik A, Kurtoğlu AE, Bilgehan M, Gülşan ME, Albegmprli HM. Support vector machines in structural engineering: A Review. J Civ Eng Manag 2015, 21(3), 261–281. https://doi.org/10.3846/13923730.2015.1005021

Dall'Aglio F. Resistenza di travi metalliche a doppio T con irrigidimenti longitudinali soggette a carichi trasversali concentrati. Doctoral dissertation. Università Degli Studi di Bologna, Dipartimento di Ingegneria Civile, Ambientale e dei Materiali, Bologna; Italy 2011 [In Italian]. http://amsdottorato.unibo.it/id/eprint/3952

Eurocode 3: Design of steel structures - Part 1-5: Plated structural elements. EN 1993-1-5: 2006.

GPlearn. Genetic Programming in Phyton with a scikit-learn inspired API, <https://gplearn.readthedocs.io/en/stable/intro.html>. Accesed in February 2023.

Graciano C, Edlund B. Failure mechanism of slender girder webs with a longitudinal stiffener under patch loading. J Constr Steel Res 2003;59(1):27–45. https://doi.org/10.1016/S0143-974X(02)00022-6.

Graciano C. Patch loading resistance of longitudinally stiffened girders–A systematic review. Thin-Walled Struct 2015, 95, 1–6. https://doi.org/10.1016/j.tws.2015.06.007

Graciano C, Kurtoglu AE, Casanova E. Machine learning approach for predicting the patch load resistance of slender austenitic stainless steel girders. Structures 2021;30:198–205. https://doi.org/10.1016/j.istruc.2021.01.012.

Hajdin N, Marković N. Failure mechanism for longitudinally stiffened I girders subjected to patch loading. Arch Appl Mech 2012;82(10):1377–1391. https://doi.org/10.1007/s00419-012-0679-4.

Kövesdi B, Mecséri BJ, Dunai L. Imperfection analysis on the patch loading resistance of girders with open section longitudinal stiffeners. Thin-Walled Struct 2018;123:195–205. https://doi.org/10.1016/j.tws.2017.11.030

Kövesdi B. Patch loading resistance of slender plate girders with longitudinal stiffeners. J Constr Steel Res 2018;140:237–246. https://doi.org/10.1016/j.jcsr.2017.10.031

Kövesdi B, Dunai L. Patch loading resistance of slender plate girders with multiple longitudinal stiffeners. ce/papers 2022, 5(4), 615-622. https://doi.org/10.1002/cepa.1798

Kurtoglu AE., Casanova E. Graciano C. Artificial intelligence-based modeling of extruded aluminum beams subjected to patch loading. Thin-Walled Struct 2022;179:109673. https://doi.org/10.1016/j.tws.2022.109673.

Loaiza N, Graciano C, Chacón R, Casanova E. Influence of bearing length on the patch loading resistance of multiple longitudinally stiffened webs. ce/papers 2017a;1(2–3):4199–4204. https://doi.org/10.1002/cepa.477

Loaiza N, Graciano C, Chacón R, Casanova E. A comparative analysis of longitudinal stiffener cross-section for slender I-girders subjected to patch loading. ce/papers 2017b;1(2–3):4223–4229. https://doi.org/10.1002/cepa.480

Loaiza N, Graciano C, Casanova E. Web slenderness for longitudinally stiffened I-girders subjected to patch loading. J Constr Steel Res 2019a;162:105737. https://doi.org/10.1016/j.jcsr.2019.105737

Loaiza N. Effect of longitudinal stiffening on the ultimate resistance of plate girders subjected to patch loading. Doctoral dissertation, Departamento de Ingeniería Civil, Universidad Nacional de Colombia, Medellín, Colombia, 2019b. https://repositorio.unal.edu.co/handle/unal/76326.

Salehi H, Burgueño R. Emerging artificial intelligence methods in structural engineering. Eng Struct 2018, 171, 170–189. https://doi.org/10.1016/j.engstruct.2018.05.084.

Shimizu S, Yoshida S, Okuhara H. An experimental study on patch loaded web plates. Proce ECCS Colloq Stab Plate Shell Struct 1987:85–94.

Schmidt MD, Lipson H. Coevolution of fitness maximizers and fitness predictors, In Proceedings of the Genetic and Evolutionary Computation Conference GECCO, Late Breaking Paper, Washington DC, 2005.

Schmidt MD, Lipson H. Learning noise. In Proceedings of the 9th Annual Conf. on Genetic and Evolutionary Computation, London, UK (2007) 1680–1685.

Sun H, Burton HV, Huang H. Machine learning applications for building structural design and performance assessment: State-of-the-art review. J Build Eng 2021, 33, 101816. https://doi.org/10.1016/j.jobe.2020.101816.

Tapeh ATG, Naser MZ. Artificial intelligence, machine learning, and deep learning in structural engineering: A scientometrics review of trends and best practices. Arch Computat Methods Eng 2023, 30, 115–159. https://doi.org/10.1007/s11831-022-09793-w.

Thai HT. Machine learning for structural engineering: A state-of-the-art review. Structures 2022, 38, 448–491. https://doi.org/10.1016/j.istruc.2022.02.003